Considering Floatting Contact and Un-Modeled Effects for Multi-Contact Motion Generation

Sébastien Lengagne, Abderrahmane Kheddar, Eiichi Yoshida

Considering Floatting Contact and Un-Modeled Effects for Multi-Contact Motion Generation

Sébastien Lengagne*, Abderrahmane Kheddar *†, Eiichi Yoshida*,
*CNRS-AIST Joint Robotics Laboratory, UMI3218/CRT, Tsukuba, Japan
†CNRS-UM2 LIRMM, Interactive Digital Human group, Montpellier, France

Abstract—In this paper, we plan robotic multi-contact non-gaited motion by solving an overall optimization problem. Our algorithm takes as input the contact stances, the model of the robot and its environment, and generates the joints trajectories that achieve multi-contact motion under explicit constraints such as joint position, velocity and torque limits, equilibrium and eventually other task objectives. We improve our previous work in order to consider floatting contacts for which some components of the contact position and/or orientation are not specified. We also discuss how, in practice, we bridge theoretical computations based on a rigid model of the robot to actual experiments by considering additional constraints during the optimization process.

Index Terms—Humanoid robots, multi-contact, floatting contact, flexibilities

I. INTRODUCTION

Recently, there has been an increasing interest in planning non-gaited motion where a humanoid robot is allowed to contact the environment with any possible part of its body to support motions in bulky and uneven spaces. For example, [1], [2] developed a contact-before-motion planning algorithm that generates a sequence of contacts for such problems. Complex examples have already been successfully experimented on a real HRP-2 robot [3]. However, in these experiments, the motion between two successive contacts, namely the transitions, was not fully dynamic. For some classes of motions, such as walking, we can use a model reduction to compute trajectories. In [4]–[6], the entire robot is assumed as an inverted pendulum having a mass or the so called cart table model. Model reduction under additional constraints allows fast motion planning from which whole body motion is generated in a latter stage. Since the generated trajectories are computed based on and for such simplified models, there is no guarantee that its expansion to whole body motion is always possible.

Multi-contact non-gaited motion uses non-stereotypical key postures. Subsequently, model reduction is not beneficial because the COMs height does not hold within a small interval range, the number of the supporting contacts varies, it is often not possible to predict non-collisions or auto-collisions, or assume that torque and joint limits will not be reached. For all these reasons, planning safe non-gaited general multi-contact motion based on models reductions is extremely difficult.

Computing dynamic motions for complex robotic systems including multiple contacts is still an open issue. Motion planning based on probabilistic methods proved to be very efficient in practice. Yet, there are tasks that require the robot to exploit dynamical effects, or reach its limits in terms of capabilities and performances. Example of such tasks are kicking motions [7], [8], fast motion with collision avoidance [9] or lifting heavy objects [10]), etc. Due to their complexity, these extreme tasks are impossible to achieve by state-of-the art planning or local control method [4], [11], [12]. Generating off-line explicit and cost optimal trajectories using full-body model is most often the only and the safest option.

Nowadays, several methods emerge to generate full body single-contact motions [8], [13]. But multi-contact motion has always been considered as separate piecewise motions between fixed contacts that are connected afterwards.
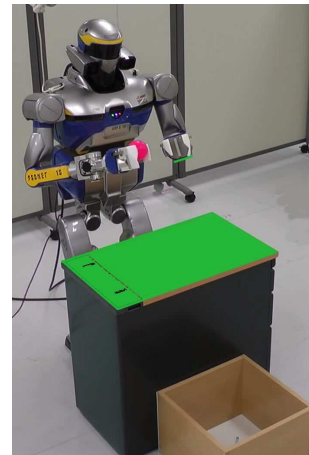

Fig. 1. The robot has to put the ball in the box behind the desk. The motion and the contact position of the left are optimized.

In our recent work [14], we proposed a method to generate full dynamic multi-contact motions between sequences of contacts, including dynamic transitions. In this paper, we propose variants to our algorithms in order to include floatting contacts, where some components of the contact position and/or orientation are not specified as presented in Figure 1. We also discuss more thoroughly the difficulty to bridge the optimization computations based on a perfect model simulation to the actual implementation and experimentation on the humanoid robot HRP-2 [15]. Despite a successfull simulations, some obtained motions were not successfully replayed in actual experiments. However, with ad-hoc tuning and addition constraints these failures could finally be recomputed and replayed successfully.

II. PROBLEM STATEMENT

Here, we introduce the basics in terms of terminology, notations, and the general formulation of the optimization problem.

A. The motion planning problem

The motion planning problem is to find the best joint trajectories $q(t)$ that minimize a cost function an ensure sets of continuous inequality constraints g, continuous equality constraints h and discrete inequality constraints z. In order to make the problem computationally solvable, most of the methods reduce such complexity by defining a parameters set $\mathbf{P} \in \mathbb{R}^N$ that give at least a parametric shape for the functions $q(t)$ to be found. Based on prior work in robotic, e.g. [13], we made the choice to shape the joint trajectories with clamped uniform cubic B-Splines curves. Subsequently, we have a finite set of B-splines'control points that constitute the set of optimization parameters. For the choice we made, we have $q_i(t) = \sum_j^m b_j^3(t) \times P_{i,j}$.

The motion planning problem reduces into finding the best parameter set $\mathbf{P} \in \mathbb{R}^N$ such that:

$$
\begin{aligned}
\underset{\mathbf{P}}{\operatorname{argmin}} \quad & C(\mathbf{P}) \\
\forall i, \forall t \in [\Delta_i] \quad & g_i(\mathbf{P}, t) \leq 0 \\
\forall j, \forall t \in [\Delta_j] \quad & h_j(\mathbf{P}, t) = 0 \\
\forall t_k \in \{t_1, t_2, ..., t_n\} \quad & z_k(\mathbf{P}, t_k) \leq 0
\end{aligned}
\tag{1}
$$

The problem 1 is called a Semi Infinite Programming (SIP) problem since it deals with a finite set of variables and a set of continuous constraint equivalent to infinite sets of constraints [16]–[18].

B. Solving SIP

In most cases, SIP is solved using a time-grid discretization of the constraints, e.g. [16]–[18]. As discussed in [7], [19], it is not easy to set *a priori* a time-grid discretization which guarantees that the constraints hold in-between a pair of sample time-point. Even if in practice, this could be checked *a posteriori*, we present another interface that accounts for continuous constraints evaluation in a guaranteed way, as presented hereafter.

We believe[1] that it is better to use a solver from on-the-shelf available ones since the theory is not enough to provide the necessary tuning and implementation tricks that tackle efficiently numerical problem. We also take this policy by using the IPOPT solver [20]. IPOPT is free; it handles large non-linear optimization problems; it has a C++ interface, and was used in [7], [8].

C. Dealing with Continuous Constraints

To solve the problem (1) without using a time-grid discretization, in [14], we ensured the joint position and velocity limits through constraints on the control points and propose a time-interval discretization within which we approximate the

---

[1]It is also very strongly suggested in all the optimization textbooks!

---

constraints and the cost function using Taylor polynomials. Thus, all the state variables of the robots are approximate over a time-interval by:

$$
\forall t \in [\Delta t] \quad f(t) \approx \sum_{i=0}^{n} a_i(\mathbf{P}) \times t^i
\tag{2}
$$

The continuous equality constraints, used to ensure constant position of the bodies during multi-contact motions, is taken into account by considering the following constraints:

$$
\forall i \in \{0, \cdots, N_e\} \quad a_i(\mathbf{P}) = 0
\tag{3}
$$

the continuous equality constraint being of order N_e Eq. (3), $N_e \leq n$ is the order that we set for the solver to avoid an over-constrained formulation (here $N_e = 2$). Note that it is also possible to consider constant value without specifying the value, as used in Section V to defined floatting contacts:

$$
\forall i \in \{1, \cdots, N_e\} \quad a_i(\mathbf{P}) = 0
\tag{4}
$$

Where the first coefficient of the polynomial is not constrained.

III. MULTI-CONTACT MOTION CONSTRAINTS

In multi-contact motion, we have to pay to attention to the geometrical constraints (to ensure the constant position of the contact bodies) and to the reaction forces (to prevent from excessive interval forces and ensure balance).

A. Geometrical constraints

To define the position of a contact body, we set two Cartesian frames; one on the contact body $\mathbf{X}_i$ and one on the environment at the desired position of the contact $\mathbf{X}_i^e$. Considering N_c contacts, we must ensure N_c sets of frame equality constraint as follows:

$$
\forall t \in [\Delta t], \forall i \in \{1, \ldots, N_c\} \quad \mathbf{X}_i(t) = \mathbf{X}_i^e
\tag{5}
$$

As we want to use floatting contacts, some component of Equation (5) refers to continuous equality constraint (Eq.(3)) and the other refers to the continuous constant constraint (Eq.(4)).

B. Inverse Dynamic Model

For each contacting link we define a set of C_i forces, and introduce the inverse dynamic model:

$$
\begin{bmatrix} \Gamma \\ 0 \end{bmatrix} = \begin{bmatrix} M_1(q) \\ M_2(q) \end{bmatrix} \ddot{q} + \begin{bmatrix} H_1(q, \dot{q}) \\ H_2(q, \dot{q}) \end{bmatrix} + \begin{bmatrix} J_1^T(q) \\ J_2^T(q) \end{bmatrix} F_c
\tag{6}
$$

where q is a vector containing the n joint position (q_i) and the position and orientation of a reference frame, Γ is the vector of size n of the torques, M the inertial matrix, H the vector due to the gravity, centrifugal and Coriolis effects, J is the Jacobian matrix and F_c is the vector of the active contact forces. In the following we note the dynamic efforts due to the dynamic of the motion: $D_2 = M_2(q)\ddot{q} + H_2(q, \dot{q})$.

C. Balance

In non-coplanar multi-contact motion, restrictive balance criteria such as the Zero Moment Point [21] do not apply. Recent work [22]–[24] propose alternative balance criteria that can deal with general non-coplanar multi-contact postures more efficiently.

For multi-contact motions, we characterize the balance by searching the contact forces that must be feasible; namely those that are necessary to hold a desired contact state, e.g. prohibiting from possible detachment or sliding of the link on the surface if not needed:

$$\forall t \in [\Delta t], \forall i \in \{1, \ldots, N_f\} \quad \begin{cases} F_i^n(t) > 0 \\ ||F_i^t(t)||^2 \leq \mu_i^2 F_i^n(t)^2 \end{cases} \tag{7}$$

where N_f is the number of contacts, F_i^n the normal component of the contact force, F_i^t the 2D vector component of the tangent force, μ_i is the friction coefficient of contact i.

D. Computation of contact forces

We compute the contact forces from the joint trajectories and a set of parameters, as shown in [14]:

$$F_i = -\mathbb{W}_i^{-1} \begin{bmatrix} \hat{P}_i A_i & A_i \end{bmatrix} \Omega^{-1} (M_2 \ddot{q} + H_2) \tag{8}$$

with $\mathbb{W}_i = \text{diag}(\beta_i \alpha_i, \beta_i \alpha_i, \beta_i)$, $\hat{P}_i$, the screw operator of the contact position, A_i the orientation of the contact framework and:

$$\Omega = \sum_i \left(\begin{bmatrix} \hat{P}_i A_i \\ A_i \end{bmatrix} \mathbb{W}_i^{-1} \begin{bmatrix} \hat{P}_i A_i & A_i \end{bmatrix} \right) \tag{9}$$

The coefficient β_i and α_i are used to modify the internal forces and can be set constant or part of the optimization variables.

In this paper, we define the coefficient α_i for all the contact forces of the same body j such that:

$$\forall i \quad \alpha_i = \frac{1000}{\mu_i \times N_i} \tag{10}$$

With N_i the number of linear contact forces acting on one body.

IV. OPTIMIZATION PROCESS

A. Decomposition of the multi-contact motion

We decompose a multi-contact motion into a set of N_p phases corresponding to the number of changes of the contact configuration, namely: breaking contact, adding contact, transition between two successive contact configurations. The duration of each phase T_i can be optimized or fixed. Moreover, to each phase corresponds a set of B-Spline basis function and each B-Spline is decomposed into several time-intervals in which the same basis function remains non null, as shown in the Fig. 2. Since we use cubic B-Splines, only four control points (that are part of the optimization parameters) influence the joint trajectory in each interval. That is, all along each time-interval any joint trajectory is under control of four control points among the total number.
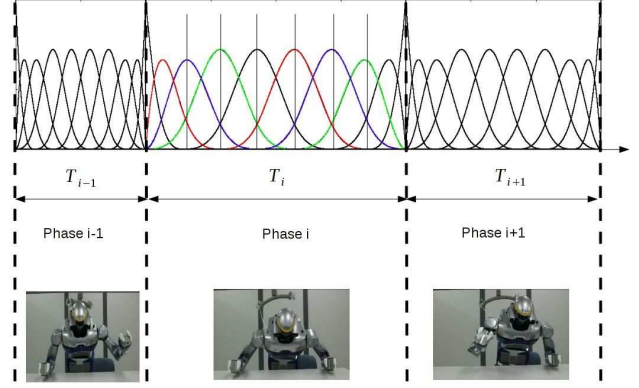

Fig. 2. Decomposition of the motion into phases and intervals. Between two phases we can break, add or maintain a contact.

The motion is defined by the optimization vector $\mathbf{P}$

$$\mathbf{P} = \left[P_{1,1}, P_{1,2}, \ldots, P_{N_{m_p}, N_p}, \beta_{1,1}, \ldots, \beta_{N_p, n_c}, T_1 \ldots, T_{N_p} \right], \tag{11}$$

where $P_{i,j}$ is the control point i of phase j, $\beta_{i,j}$ is the force coefficient of the contact i of phase j, and T_i is the time duration of phase i.

We enforce the joint position, velocity and acceleration continuity by computing the three first control points of phase $j \in [2, \cdots, N_p]$ from the three last control points of the previous phase $j-1$. Then, we compute the constraints on each interval to feed the optimization solver, at each step. Since we use the inverse dynamic model, the computation for one interval is fully independent from the other ones. Subsequently, we use multi-threading to reduce the computation time.

In this paper, we get rid of the impact model and the switching among model (which otherwise turn to be a hybrid system) by considering perfectly inelastic contact. This is plausible as long as the muti-contact motion is made with contact breaking and creation at zero to low speeds (which is the case of our motions).

B. Set of Constraints

We consider humanoid robots as rigid bodies, with N_{dof} degrees of freedom (dof). To produce safe motions, we check for the joint position, velocity and torque limit all along the motion duration $\forall t \in [0, T]$:

$$\forall k \in \{1, \ldots, N_{dof}\} \quad \begin{cases} \underline{q_k} \leq q_k(t) \leq \overline{q_k} \\ \underline{\dot{q}_k} \leq \dot{q}_k(t) \leq \overline{\dot{q}_k} \\ \underline{\Gamma_k} \leq \Gamma_k(t) \leq \overline{\Gamma_k} \end{cases} \tag{12}$$

The balance is ensured by considering no-sliding constraints (cf. Eq. (7)), which are gathered into a unique constraint for each contact forces F_i:

$$F_{i,x}(t)^2 + F_{i,y}(t)^2 - \text{sign}(F_{i,z}) \times \mu_i^2 F_{i,z}(t)^2 \leq 0 \tag{13}$$

The Equation (13) cannot be satisfied if $F_{i,z} < 0$ or if the force is not within the friction cone. Unfortunately, the function

sign($F_{i,z}$), is not continuous, in order to allow a polynomial approximation, we replace it by $\frac{2}{\pi} \operatorname{atan}(F_{i,z})$.

Then, in order to interface all the constraints with the optimization solver, we gather them into a set of inequality constraints:

$$\forall i, \forall t \in [0, T] \quad g_i(q(t), \dot{q}(t), \ddot{q}(t)) \leq 0 \qquad (14)$$

We note N_g the total number of constraints, which includes the continuous inequality $g(\mathbf{P})$, the equality $h(\mathbf{P})$ and the discrete inequality $z(\mathbf{P}, t_k)$ used by the optimization solver.

C. Cost function

For humanoid robots, one can find a lot of different cost functions, depending on the robot performances and desired task. Nevertheless, it is not easy to guess the cost function that human beings minimize during their motions. In order to get human-like motion, we tried several cost functions: minimum jerk for smooth motion, minimum time for fast motion, minimum energy consumption. Eventually, in this paper, we consider a combination of these three criteria:

$$C = \sum_{i=1}^{N_p} aT_i + \sum_{i=1}^{N_{dof}} \int_0^T \left(b\Gamma_i^2 + c\ddot{q}_i^2 \right) dt \qquad (15)$$

We heuristically found $a = 5$, $b = 10^{-2}$, $c = 10^{-6}$.

V. FREE CONTACT POSITION

In order to assess the validity of our approach, we already designed experiments on a real humanoid platform: the HRP-2 robot [15]. In [14], we produced kicking motions with and without hand contact and a sitting motion, where the robot perform several contact on the table in order to sit on the chair. In [25], we reproduced walking motion emulating leg injuries and diseases by adding some constraints on the knee joint position or limits on contact forces.

In this paper, we extend our work by taking into account floatting contacts, where some components of the contact position and/or orientation are not fixed and optimized during the motion generation. Since the contact stance are given based on static postures [2], they can lead to unfeasible motion and their position may need to be different, thus to be optimized.

To emphasize the effectiveness of our method, we generate a motion where the robot has to lean on a table with its left hand in order to put an object in a trash located behind the table. The x and y-position and z-orientation of the left hand is not given and are optimized. Eventually, we get the motion presented in Figure 3 with the left hand located at $x = 50cm, y = 0.19cm$ and $\theta_z = -0.5rad$ regarding to the world frame located between the foot.

The Figure 4 shows the contact force measured by the force sensors during the real experiments. Unfortunately, the robot does not have force sensor to measure the contact forces applied on the left hand. Nevertheless, the sum of the two contact forces of the foot (blue line on Figure 4) gives us some indications about it, since it does not compensate the total weight of the robot. This emphasize the effects of the left hand contact forces.
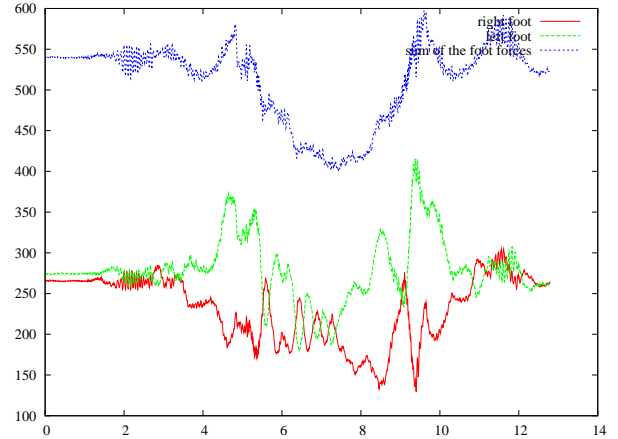

Fig. 4.   Time history of the contact forces during the motion

VI. FROM PERFECT MODEL TO ACTUAL EXPERIMENTS

In this section, we experiment a walking motion overcrossing a fifteen-centimeter platform. During the first experiment of the walking motion on the fifteen-centimeter platform, after passing over the platform, the landing foot induces an impact such that it generated an entire (small) hop of the robot as shown in Figure 5; although this was not observed in simulation.

Fig. 5.   The robot makes a hop after landing the left foot (the feet does not touch the ground in the middle picture and the robot is not in contact anywhere.)

Indeed this motion emphasize the difficulties to bridge off-line model-based motion planning computations to actual robotic experiments. Unfortunately, during real experiments. We formulate the multi-contact motion generation as an optimization problem. The cost function and the constraints are explicitly or implicitly written based on a perfect model of the robot. We considered the HRP-2 as a poly-articulated system made of rigid links and perfect links, that is, no uncertainties and no flexibility. However, the robot is equipped with a shock absorbing mechanism, placed at the ankle, and which is by design flexible in order to limit the effects of impact forces due contacts of the leg with the ground during walking or running.

Unfortunately, this system is equivalent to a non-controllable joint that influences the attitude behavior of the robot, especially during contact creation and release. To deal with this problem, it is possible to use a stabilizer such as the one proposed in [26], [27], i.e., a control loop that compensate for these flexibilities and even light external perturbations.
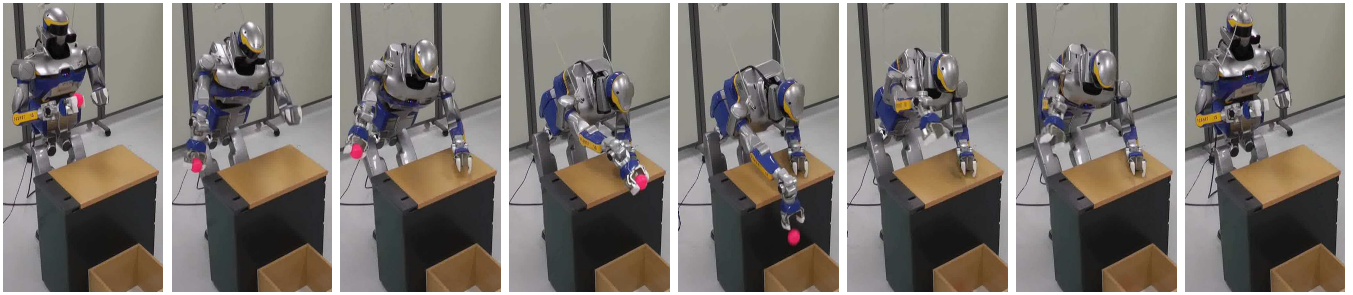
Fig. 3. The HRP-2 leans its left hand on a desk to put a ball in a box behind the desk. The motion and the position and orientation of the left hand contact are obtained by our method.

Nevertheless, the stabilizer as it is conceived now on the HRP-2 cannot deal with some motions such as those shown on Figure 5.
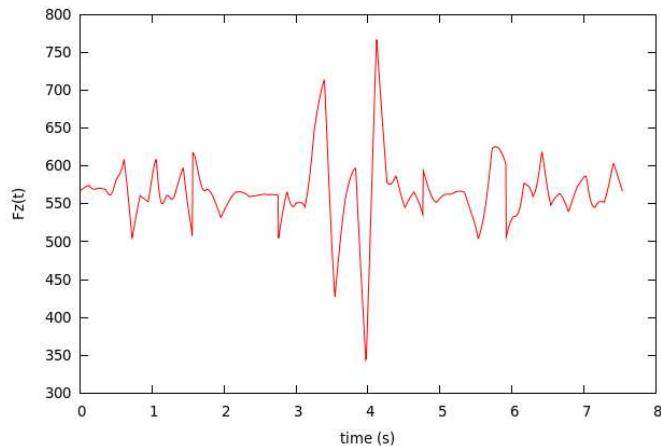

Fig. 6. Time history of the vertical component of the free dynamics effect D_2

Figure 6 shows the time history of the vertical component F_z of the free dynamic force D_2 that must be counterpart by the contact forces. We see that there is a large variation of this force during the platform passing over. We assume that this force (more than 125% of the force in static posture) introduces an energy that is stored as a deformation potential of the flexible shock absorbing mechanism. When this force is suddenly reduced at landing time, the stored energy is released which produces a hop. To avoid this phenomena, we added a constraint on the normal component F_z of D_2 during the optimization process:

$$\forall t \in [\Delta t] \qquad 560 \leq F_z(t) \leq 580 \qquad (16)$$

Eventually, we successfully perform the experiment as shown in Figure 7.

In summary, by ad-hoc restraining the free dynamic effects we can generate a walking motion that can be performed during real experiments without any hop due to ankle flexibilities. Even if the stabilizer is very effective for walking motions, it is based on a set of assumptions that is very limitative and cannot fit with all the motions the robot can actually perform.

VII. DISCUSSION

In this paper, we propose a method to generate multi-contact motions in full-body dynamics. We assessed its effectiveness by demonstrating some challenging experiments using the HRP-2 humanoid robot. The one presented here constitute a sample of all the motions we computed under other conditions or cost functions. Moreover, these experiments proved to be repeatable at will. The videos of all the experiments we performed are available on the website [28].

Some of the motions we computed produce collision between the robot and the environment or often self-collision. In the presented motion, we had added artificial constraints to avoid this phenomena. As an urgent work, we need to integrate collision avoidance constraints, which require a thorough investigation because the problem is far from being simple. Actually we are already working on a solution to evaluate the distance function on the entire time interval and extend the safe advanced techniques proposed in the computer graphics community [29]. This method works by assuming a constant velocity between two time samples, we are working on getting ride of this and we are confident to reach a satisfactory solution. However, we realized that the metrics, which is used to evaluate the distance function, might be not well posed from the mathematical basis viewpoint. Another problem is that such constraints will certainly increase the non-convexity of the problem that need to be considered.

VIII. CONCLUSION

In this paper, we present a method to generate multi-contact dynamical and non-gaited motions. First, the motion planning is formulated as an optimization problem with a set of continuous constraints that describes the motion, the limitations of the robot and a cost function. We handle those continuous constraints using a polynomial approximation and ensure their validity all along the motion. We proposed some improvment in order to consider floatting contact for which some components of the contact position and/or orientation are not specified and discussed how, in practice, we bridge theoretical computations based on a rigid model of the robot

Fig. 7. The HRP-2 overcrossing a fifteen-centimeter platform: the HRP-2 takes steps the platform with one foot and over-cross it with the other.

to actual experiments by considering additional constraints during the optimization process.

To asses our method, we compute several dynamical motions to highlight the effectiveness and the robustness of our method. We developed a method to produce generic motions that cannot be generated by state-of-the-art methods using only contact between the foot and the ground. We will also work on adding sliding contacts in order to generate some tasks motions such as cleaning a table or a board and considering free floating motion such as running or jumping.

REFERENCES

[1] K. Hauser, T. Bretl, and J. C. Latombe, "Non-gaited humanoid locomotion planning," in *Humanoid Robots, 2005 5th IEEE-RAS International Conference on*, Tsukuba,, Dec. 2005, pp. 7–12.

[2] K. Bouyarmane, A. Escande, F. Lamiraux, and A. Kheddar, "Potential field guide for humanoid multicontacts acyclic motion planning," in *IEEE International Conference on Robotics and Automation*, may 2009.

[3] A. Escande and A. Kheddar, "Contact planning for acyclic motion with tasks constraints," in *IEEE/RSJ International Conference on Intelligent RObots and Systems (IROS 2009)*, Oct. 11-15 2009.

[4] S. Kajita, F. Kanehiro, K. Kaneko, K. Fujiwara, K. Harada, K. Yokoi, and H. Hirukawa, "Biped walking pattern generation by using preview control of zero-moment point," in *IEEE International Conference on Robotics and Automation*, vol. 2, september 2003, pp. 1620 – 1626.

[5] ——, "Resolved momentum control: Humanoid motion planning based on the linear and angular momentum," in *Intl. Conference on Intelligent Robots and Systems*, 2003.

[6] S. Lee and A. Goswami, "Reaction mass pendulum (RMP): An explicit model for centroidal angular momentum of humanoid robots," in *IEEE International Conference on Robotics and Automation (ICRA)*, april 2007, pp. 4667–4672.

[7] S. Lengagne, N. Ramdani, and P. Fraisse, "Planning and fast replanning safe motions for humanoid robots," *IEEE Transaction on RObotics*, vol. 27, december 2011.

[8] S. Miossec, K. Yokoi, and A. Kheddar, "Development of a software for motion optimization of robots: Application to the kick motion of the HRP-2 robot," in *IEEE International Conference on Robotics and Biomimetics*, 2006, pp. 299–304.

[9] A. I. F. Vaz, E. M. Fernandes, and M. P. S. Gomes, "Robot trajectory planning with semi-infinite programming," *European Journal of Operational Research.*, vol. 153, no. 3, pp. 607–617, 2004.

[10] H. Arisumi, S. Miossec, J.-R. Chardonnet, and K. Yokoi, "Dynamic lifting by whole body motion of human robots," in *IEEE/RSJ International Conference on Intelligent Robots and Systems (IROS)*, september 2008, pp. 668–675.

[11] P.-B. Wieber, "Trajectory Free Linear Model Predictive Control for Stable Walking in the Presence of Strong Perturbations," in *IEEE-RAS International Conference on Humanoid Robots*, Genova Italie, 2006.

[12] L. Sentis, J. Park, and O. Khatib, "Compliant control of multicontact and center-of-mass behaviors in humanoid robots," *IEEE Transactions on robotics*, vol. 26, pp. 483–501, 2010.

[13] S.-H. Lee, J. Kim, F. Park, M. Kim, and J. E. Bobrow, "Newton-type algorithms for dynamics-based robot movement optimization," in *IEEE Transactions on robotics*, vol. 21, 2005, pp. 657– 667.

[14] S. Lengagne, A. Kheddar, and E. Yoshida, "Generation of optimal dynamic multi-contact motions: Application to humanoid robots." *IEEE Transactions on robotics*, vol. ??, p. ??, 2011, submitted.

[15] K. Kaneko, F. Kanehiro, S. Kajita, H. Hirukawa, T. Kawasaki, M. Hirata, K. Akachi, and T. Isozumi, "Humanoid robot HRP-2," in *IEEE International Conference on Robotics and Automation*, vol. 2, Apr./May 2004, pp. 1083–1090.

[16] R. Reemtsen and J.-J. Rückmann, *Nonconvex optimization and its applications : Semi-infinite Programming*, R. Reemtsen and J.-J. Rückmann, Eds. Kluwer Academic Publishers, 1998.

[17] O. Von Stryk, "Numerical solution of optimal control problems by direct collocation," in *in Optimal Control, (International Series in Numerical Mathematics 111*, 1993, pp. 129–143.

[18] R. Hettich and K. O. Kortanek, "Semi-infinite programming: theory, methods, and applications," *SIAM Rev.*, vol. 35, no. 3, pp. 380–429, 1993.

[19] O. Von Stryk and R. Bulirsch, "Direct and indirect methods for trajectory optimization," *Ann. Oper. Res.*, vol. 37, no. 1-4, pp. 357–373, 1992.

[20] A. Wächter and L. T. Biegler, "On the implementation of a primal-dual interior point filter line search algorithm for large-scale nonlinear programming," *Mathematical Programming*, vol. 106, pp. 22–57, 2006.

[21] M. Vukobratović, "On the stability of anthropomorphic systems," *Mathematical Biosciences*, vol. 15, pp. 1–37, 1972.

[22] P.-B. Wieber, "On the stability of walking systems," in *Proceedings of the International Workshop on Humanoid and Human Friendly Robotics*, Tsukuba, Japan, 2002.

[23] H. Hirukawa, S. Hattori, K. Harada, S. Kajita, K. Kaneko, F. Kanehiro, K. Fujiwara, and M. Morisawa, "A universal stability criterion of the foot contact of legged robots - adios ZMP," in *IEEE International Conference on Robotics and Automation (ICRA).*, may 2006, pp. 1976– 1983.

[24] T. Bretl and S. Lall, "Testing static equilibrium for legged robots," *IEEE Transactions on Robotics*, vol. 24, no. 4, pp. 794–807, Aug. 2008.

[25] S. Lengagne, A. Kheddar, S. Druon, and E. Yoshida, "Emulating human leg impairments and disabilities in walking with humanoid robots," in *IEEE International Conference on Robotics and Biomimetics*, 2011, submitted.

[26] S. Kajita, T. Nagasaki, K. Kaneko, K. Yokoi, and K. Tanie, "A running controller of humanoid biped HRP-2LR," in *IEEE International Conference on Robotics and Automation*, Apr. 2005, pp. 616–622.

[27] K. Kaneko, K. Komoriya, K. Ohnishi, and K. Tanie, "Manipulator control based on a disturbance observer in the operational space," in *IEEE International Conference on Robotics and Automation*, vol. 2, 1994, pp. 902–909.

[28] [Online]. Available: http://staff.aist.go.jp/sebastien.lengagne/videos.html

[29] X. Zhang, S. Redon, M. Lee, and Y. J. Kim, "Continuous collision detection for articulated models using taylor models and temporal culling," *ACM Trans. Graph.*, vol. 26, no. 3, p. 15, 2007.